

# Blood-derived iron mediates free radical production and neuronal death in the hippocampal CA1 area following transient forebrain ischemia in rat

Ui Jin Park · Young Ae Lee · Sun Mi Won · Jin Hwan Lee · Seung-Hee Kang ·  
Joe E. Springer · Yong Beom Lee · Byoung Joo Gwag

Received: 30 August 2010 / Revised: 18 November 2010 / Accepted: 18 November 2010  
© Springer-Verlag 2010

**Abstract** Abnormal brain iron homeostasis has been proposed as a pathological event leading to oxidative stress and neuronal injury under pathological conditions. We examined the possibility that neuronal iron overload would mediate free radical production and delayed neuronal death (DND) in hippocampal CA1 area after transient forebrain ischemia (TFI). Mitochondrial free radicals (MFR) were biphasically generated in CA1 neurons 0.5–8

and 48–60 h after TFI. Treatment with Neu2000, a potent spin trapping molecule, as well as trolox, a vitamin E analogue, blocked the biphasic MFR production and attenuated DND in the CA1, regardless of whether it was administered immediately or even 24 h after reperfusion. The late increase in MFR was accompanied by iron accumulation and blocked by the administration of deferoxamine—an iron chelator. Iron accumulation was attributable to prolonged upregulation of the transferrin receptor and to increased uptake of peripheral iron through a leaky blood–brain barrier. Infiltration of iron-containing cells and iron accumulation were attenuated by depletion of circulating blood cells through X-ray irradiation of the whole body except the head. The present findings suggest that excessive iron transported from blood mediates slowly evolving oxidative stress and neuronal death in CA1 after TFI, and that targeting iron-mediated oxidative stress holds extended therapeutic time window against an ischemic event.

U. J. Park · S. M. Won · J. H. Lee · Y. B. Lee (✉) · B. J. Gwag  
Neuroscience Graduate Program, Ajou University School  
of Medicine, San 5, Wonchun-Dong, Yeoungtong-Gu,  
Suwon 443-749, South Korea  
e-mail: yblee@ajou.ac.kr

B. J. Gwag (✉)  
Department of Pharmacology, Ajou University School  
of Medicine, San 5, Wonchun-Dong, Yeoungtong-Gu,  
Suwon 443-749, South Korea  
e-mail: bjgwag@ajou.ac.kr; bjgwag5001@gmail.com

Y. B. Lee  
Institute For Medical Science, Ajou University School  
of Medicine, Suwon 443-749, South Korea

U. J. Park · Y. A. Lee · J. H. Lee · B. J. Gwag  
Neurotech Pharmaceuticals Co. Ltd., Ajou University Hospital,  
Suwon 443-749, South Korea

S.-H. Kang  
Department of Radiation Oncology, Ilsan-Paik Hospital,  
Inje University College of Medicine, Goyang 411-706,  
South Korea

J. E. Springer  
Department of Physical Medicine and Rehabilitation,  
University of Kentucky, Lexington, KY, USA

J. E. Springer  
Spinal Cord and Brain Injury Research Center,  
University of Kentucky, Lexington, KY, USA

**Keywords** Iron · Blood–brain barrier · Free radicals ·  
Transferrin receptor · CA1 pyramidal neurons ·  
Transient forebrain ischemia

## Introduction

A brief period of global cerebral ischemia, occurring in patients during cardiac arrest or induced experimentally in animals, causes the selective degeneration of CA1 pyramidal neurons in the hippocampus 2–4 days after reperfusion [27, 49, 59]. Three plausible hypotheses have been proposed as key mechanisms underlying this delayed neuronal death (DND) after transient forebrain ischemia (TFI). First,  $Ca^{2+}$ -permeable  $\alpha$ -amino-3-hydroxy-

5-methyl-4-isoxazolepropionic acid (AMPA) glutamate receptors can mediate DND through the downregulation of glutamate receptor 2 (GluR2), a  $\text{Ca}^{2+}$ -impermeable AMPA receptor subunit, in CA1 neurons after TFI, resulting in the formation of  $\text{Ca}^{2+}$ -permeable AMPA glutamate receptors [2, 45]. Excess  $\text{Ca}^{2+}$  influx and accumulation then triggers degeneration of CA1 neurons [15]. In support of this, administration of the AMPA receptor antagonist NBQX or the calcium channel blockers KB-2796 or 1-naphthyl acetyl spermine (Naspm) reduces DND [42, 54, 60]. Second,  $\text{Zn}^{2+}$  influx and accumulation in CA1 neurons can contribute to DND through the translocation of  $\text{Zn}^{2+}$  from presynaptic terminals into CA1 neurons following TFI, leading to neuronal death possibly by triggering mitochondrial depolarization and extracellular signal-regulated kinase activation [21, 28, 35]. Blockade of rising intracellular  $\text{Zn}^{2+}$  in CA1 neurons with the zinc chelators calcium EDTA or *N,N,N',N'*-tetrakis(2-pyridylmethyl)ethylenediamine attenuates DND [4, 28]. Finally, the reduction of free radicals has been shown to protect hippocampal CA1 neurons from TFI [16, 55], suggesting that free radicals comprise an additional route to DND [6, 20, 57].

Iron overload has been implicated in free radical production and neuronal death in neurodegenerative diseases including Alzheimer's disease (AD) and Parkinson's disease (PD), and in stroke [5, 33, 44, 53, 61]. Under these pathological conditions, iron released from iron-binding proteins such as ferritin and cytochromes can catalyze free radical reactions by Fenton chemistry and Haber–Weiss cycle, resulting in damage to all types of biomolecules [24, 31, 39]. In fact, lipid, DNA, and protein oxidation by iron-catalyzed reactive-oxygen species (ROS) such as hydroxyl radicals and peroxy/alkoxy radicals is evident by elevated levels of malondialdehyde, 4-hydroxynonenal, isoprostanes, 8-hydroxyguanine in the blood and/or brain in AD, PD, and stroke [1, 7, 34, 36, 58].

Administration of deferoxamine, an iron chelator, was shown to reduce brain lipid peroxidation, neurological injury, and mortality in dog or rat subjected to transient cardiac arrest [29, 41, 51]. In rat, TFI caused late-onset iron overload in the CA1 area after 4 weeks that paralleled appearance of reactive astrocytes and ferritin-immunoreactive microglia [30]. This raises a possibility that iron may mediate free radical generation and DND in CA1 pyramidal neurons following TFI. To test this hypothesis, we first conducted experiments to delineate the causal relationship between iron overload, free radical generation, and neuronal death in CA1. We further investigated if iron regulatory proteins and iron transport through blood–brain barrier (BBB) opening would participate in altered iron homeostasis in CA1 neurons.

## Materials and methods

### Animals

Sprague–Dawley rats (male, 250–300 g) and fetal ICR mice were purchased from Orient Bio Inc. (Seoungnam, Korea) for all experiments. All experimental procedures were conducted under the approval of the Institutional Animal Care and Use Committee of Ajou University School of Medicine.

### Transient forebrain ischemia

TFI was induced by four-vessel occlusion with minor modifications of the method previously described [47, 48]. The four-vessel occlusion method of inducing ischemia involves cauterization of both vertebral arteries plus transient occlusion of the carotid and results in significant reduction of the cerebral blood flow (90% or more) [43]. Briefly, rats were anesthetized with chloral hydrate (400 mg/kg, i.p.), and bilateral vertebral arteries were exposed and electrocauterized, followed by isolation of both common carotid arteries (CCAs) and placing polyethylene tube (PE-10) loosely around the CCAs. After 24 h, the CCAs were occluded bilaterally using aneurysm clips for 10 min. The body temperature was monitored by rectal thermistor probe and maintained at  $37.5 \pm 0.5^\circ\text{C}$  with heating pads during ischemia and until animals were completely recovered. Animals were fasted for 1 day before the induction of ischemia and thereafter they were allowed free access to food and water. Sham-operated animals were treated identically except that vertebral arteries and CCAs were not occluded. The total number of rats was 240 in the present study, while 25 rats died either during surgical procedure or occlusion of forebrain ischemia. Death was not observed following reperfusion or sham operation. Animals were grouped as follows: 120 rats for the analysis of mitochondrial free radicals (MFR), 44 rats for cell death analysis, 24 rats for histochemistry, 12 rats for Evans blue injection, and 15 rats for irradiation.

### Drug treatment

Neu2000 (Neurotech Pharmaceuticals Co., Ltd., Korea) and trolox (Sigma) were injected immediately or 24 h after reperfusion at a dose of 50 mg/kg (i.p). Deferoxamine mesylate (DFO, Sigma) was administered subcutaneously (s.c.) immediately after reperfusion at a dose of 100 mg/kg. Ca-EDTA (100 mM) was administered using a stereotaxic apparatus (Kopf Instruments, Tujunga, CA) into the left lateral ventricle (i.c.v.) at a flow rate of 1  $\mu\text{l}/\text{min}$  for 5 min, at the onset of reperfusion. Control rats received saline (0.9% NaCl) as a vehicle. Five rats were used for each

group except that six rats were used for post-treatment group with Neu2000, cell death analysis at 7 days after administration of deferoxamine, and cell death analysis at 3 days after TFI.

#### Tissue preparation

Animals were killed and subjected to trans-cardiac perfusion with phosphate buffered saline (PBS, pH 7.4) and 4% paraformaldehyde. For analysis of circulating blood cells in the brain, animals were directly subjected to trans-cardiac perfusion with 4% paraformaldehyde. Brains were removed, stored in 4% paraformaldehyde at 4°C overnight, and immersed in 30% sucrose for 3–4 days at 4°C. The brains were then frozen rapidly in powdered dry ice and stored at –70°C. The frozen brains were sectioned coronally between 3 and 4 mm posterior to the bregma to a thickness of 25 µm using a Cryocut Microtome (Leica Microsystems, Wetzlar, Germany) and stored in stock solution [0.1 M phosphate buffer pH 7.4, 30% (v/v) glycerol, 30% ethylene glycol] at 4°C until use.

#### Immunohistochemistry

Free-floating sections were incubated in 0.3% H<sub>2</sub>O<sub>2</sub> and 0.25% Triton X-100 for 10 min at room temperature and treated with 10% normal goat serum for 1 h. Sections were then incubated with one of the following primary antibodies: mouse anti-NeuN (diluted 1:200, Chemicon International, Temecula, CA), mouse anti-transferrin receptor (anti-TfR, diluted 1:200, Zymed Laboratories Inc., San Francisco, CA), polyclonal rabbit anti-human Transferrin (diluted 1:200, DakoCytomation., Glostrup, Denmark), biotin-conjugated rabbit anti-ferritin (diluted 1:200, Abcam, Cambridge, UK), polyclonal rabbit anti-human myeloperoxidase (MPO, diluted 1:50, DakoCytomation., Glostrup, Denmark), mouse anti-rat CD163 (ED2; diluted 1:100, Serotec Inc., Oxford, England), fluorescein isothiocyanate-labeled anti-human glycophorin A (diluted 1:10, Invitrogen Corp., CA, USA), mouse anti-EBA (endothelial barrier antigen) (diluted 1:1,000, SMI 71, Sternberger Monoclonals, Lutherville, MD, USA). After 24 h, the sections were thoroughly washed with PBS, incubated with fluorescein isothiocyanate-labeled horse anti-mouse IgG (diluted 1:200, Vector Laboratories, Burlingame, CA), Texas Red goat anti-rabbit IgG (diluted 1:200, Vector Laboratories), Rhodamine avidin D (diluted 1:200, Vector Laboratories) or AMCA streptavidin (diluted 1:200, Vector Laboratories) for 2 h at RT, washed again with PBS, and mounted on gelatin-coated slides. Double immunolabeling was carried out by reaction with the first primary antibody which was followed by reaction with the second primary antibody pre-conjugated to each

fluorescent-labeled secondary antibody by *in vitro* incubation [9]. For 8-OHdG (a marker of oxidative stress to DNA) detection, the avidin–biotin complex technique followed by DAB staining was used. Primary antibody was monoclonal mouse anti-8-OHdG antibody (10 µg/ml; Oxis International Inc., Portland, Ore). Normal mouse IgG (Vector Laboratories) was used as negative control. The secondary antibody was anti-mouse IgG (diluted 1:200, Vector Laboratories).

#### Quantitation of neuronal death in the CA1

Delayed neuronal degeneration was assessed by histological examination of Cresyl violet-stained brain sections at the level of the dorsal hippocampus collected from animals killed 3 or 7 days after ischemia as previously reported [57]. For quantitative analysis, surviving neurons in the CA1 layer within a 50 × 200 µm rectangular area were counted using an ocular grid within the microscope eyepiece (Olympus Optical Co., Tokyo, Japan). The mean number of surviving cells in three non-adjacent sections was calculated for each animal. We routinely performed counting of surviving neurons in a blind manner.

#### Detection and analysis of MFR

MFR (5 rats for each group) were analyzed using MitoTracker Red CM-H<sub>2</sub>XRos as previously described [25]. Animals were anesthetized with chloral hydrate (400 mg/kg, *i.p.*), placed into a Kopf stereotaxic apparatus, and injected with 0.4 nmol MitoTracker Red CM-H<sub>2</sub>XRos into the lateral ventricle 1 day prior to TFI induction. Animals were euthanized and perfused transcardially with PBS and 4% paraformaldehyde. The brains were removed, fixed, and sectioned at a thickness of 25 µm. The sections were subjected to immunohistochemistry with mouse anti-NeuN and Hoechst 33258 (Sigma) to label neurons and nuclei, respectively. MFR were analyzed by monitoring the oxidized fluorescence product (excitation 554 nm, emission 576 nm) of MitoTracker Red CM-H<sub>2</sub>XRos under a fluorescence microscope equipped with a cooled CCD system (CoolSNAP monochrome cf/OL, Olympus). The fluorescent intensity of MitoTracker Red CM-H<sub>2</sub>XRos in hippocampal neurons was measured using MetaMorph image analysis software (Universal Imaging Corporation, USA).

#### Iron histochemistry with Perl's staining

Iron staining was performed according to a 3,3'-diaminobenzidine tetrahydrochloride (DAB)-enhanced method of Prussian Blue staining [22, 32]. In brief, sections were

washed with distilled water and immersed in Perl's solution containing 2% potassium ferrocyanide and 2% hydrochloric acid for 30 min. The sections were washed and then incubated in 0.05% DAB solution in 0.1 M phosphate buffer (pH 7.4) and followed by addition of hydrogen peroxide (0.5 ml of 1% H<sub>2</sub>O<sub>2</sub> to 100 ml DAB solution). No signal was observed in sections subjected to the DAB intensification procedure without prior incubation with Perl's solution. The number of iron-positive cells was analyzed in the CA1 subfields containing brain capillary endothelium from three brain sections of each animal. Iron stain-positive cells were counted on 400-fold magnification images using the manual counting module using MetaMorph image analysis software (Universal Imaging Corporation, USA). The iron intensity was analyzed via pixel-quantification of signal positive to Perl's staining in the CA1 cells on 400-fold magnification images using the Image Gauge software (FUJIFILM Science Lab Image Gauge Ver. 4.0.)

#### Zinc staining

Intracellular zinc was visualized using 6-methoxy-8-quinolyl-para-toluenesulfonamide (TSQ), a membrane-permeable zinc-chelating dye [11]. Cultured cells were incubated in a solution of 4.5  $\mu$ M TSQ (Molecular Probes, Eugene, OR) in 140 mM sodium barbital and 140 mM sodium acetate buffer, pH 10. After 5 min, the sections were washed with PBS and observed under a fluorescence microscope with an ultraviolet filter (excitation 365 nm, dichroic mirror 400 nm, barrier 450 nm).

#### Extravasation of Evans blue dye (EBD)

BBB permeability (3 rats for each group) was investigated by monitoring the extravasation of EBD. The EBD-albumin conjugate can be identified macroscopically by its striking blue color within tissue and observed by red auto-fluorescence in tissue sections examined by fluorescence microscopy [40]. Sham-operated animals or ischemic/reperfused animals were injected with 0.1 ml of 4% EBD (Sigma) in 0.9% saline through a dissected femoral vein. After 30 min, animals were killed by transcardial perfusion using 200 ml PBS. The brains were removed, fixed with paraformaldehyde, and sectioned at a thickness of 25  $\mu$ m. The sections were incubated for 30 min with fluorescein-*Lycopersicon esculentum* (Tomato) Lectin (Vector Laboratories) to label brain capillary endothelial cells, rinsed with PBS, and then mounted. The extravasation of Evans blue was observed under a fluorescent microscope (excitation 557 nm, emission 576 nm).

#### X-ray irradiation

X-ray irradiation to total body was performed to suppress hematopoiesis, resulting in depletion of circulating blood cells including leukocytes and lymphocytes [23]. Animals were anesthetized with chloral hydrate (400 mg/kg i.p.) and placed in the supine position. Animals (5 rats for each group) were irradiated with a single dose of 650 cGy using a 6-MV photon beam (CLINAC 2100C/D, Varian Medical System). Irradiation was delivered to the whole body excluding the head with anterior and posterior opposing fields at a distance of 100 cm from source to axis. Blood samples were collected from the femoral vein 5 days after irradiation, and blood cells were counted using a Hemavet 950 FS (Drew Scientific Inc., USA).

#### Primary cortical cell culture and lactate dehydrogenase (LDH) assay

Cortical cells were obtained from the brains of fetal ICR mice at 14–15 gestational days and plated (approximately  $2.5 \times 10^5$  cells per well) either in 24-well plates to examine the effects of oxidative stress on neuronal survival or on plastic coverslips for immunohistochemistry pre-coated with plating media consisting of Eagle's minimal essential media (MEM, Earle's salts, supplied 100  $\mu$ g/ml poly-D-lysine and 4  $\mu$ g/ml laminin, glutamine-free, GIBCO, USA) supplemented with 5% horse serum, 5% fetal bovine serum, 2 mM glutamine, and 21 mM glucose. Cultures were maintained at 37°C in a humidified 5% CO<sub>2</sub> atmosphere. For co-cultures of neurons and glia, 10  $\mu$ M cytosine arabinofuranoside was added to cultures at 7–9 days in vitro (DIV) when glial cells were confluent beneath neurons. Cultures were fed with growth medium without fetal bovine serum twice per week until experiments. Neuronal damage was observed under a phase contrast microscope following oxidative challenges. Neuronal death was analyzed as previously described [17]. Mixed cortical cell cultures (13–15 DIV) were subjected to oxidative stress by continuous exposure to FeCl<sub>2</sub>, menadione, or H<sub>2</sub>O<sub>2</sub>, or by 30-min exposure to ZnCl<sub>2</sub> in MEM containing 25 mM glucose. Oxidative neuronal death was analyzed 24 h later by measuring the amount of LDH released into bathing media.

#### Statistical analysis

All data are normalized to control values considered as 100%, and the results are expressed as mean  $\pm$  SEM. Statistical analysis was performed using Student's *t* test and one-way ANOVA followed by Student–Newman–Keuls test (SPSS, Chicago, IL). *P* values <0.05 were

considered statistically significant and are indicated as asterisks or hash symbols in figures.

## Results

The biphasic pattern of free radical production in CA1 pyramidal neurons following TFI

We first investigated the temporal pattern of MFR production in the hippocampal formation following TFI by monitoring the oxidized fluorescent products of Mito-Tracker Red CM-H2TMRos as previously reported [25]. MFR were detectable at low levels in the dentate gyrus of sham-operated rat brains. Levels of MFR were high in the pyramidal cell layers compared to the dentate gyrus. The fluorescence intensity of MFR increased significantly in CA1 pyramidal neurons ( $P < 0.05$ ), but not in dentate gyrus granule cells, 2 h after TFI (Fig. 1a). MFR levels in CA1 neurons increased from 0.5 to 8 h, returned to control levels from 16 to 36 h, and then increased again from 48 to 60 h after TFI (Fig. 1b). MFR production returned to control levels after 72 h in conjunction with delayed degeneration of CA1 neurons. The biphasic patterns of oxidative stress in the CA1 neurons were further verified by increased immunoreactivity to 8-hydroxyl-deoxyguanosine (8-OHdG), a marker of oxidation of DNA, at 2 and 48 h after TFI (Fig. 1c).

The extended neuroprotective time window of antioxidants against DND

Neu2000 is a potent spin trapping molecule that completely blocks  $\text{Fe}^{2+}$ -induced free radical toxicity at 300 nM in cultured cortical neurons [18]. Administration of Neu2000 (50 mg/kg, ip) significantly blocked MFR production in CA1 neurons 2 h and 2 days after TFI (Fig. 2a, b). Trolox (50 mg/kg, ip), a water-soluble form of alpha-tocopherol, also reduced TFI-induced free radical production (Fig. 2b). Treatment with Neu2000 substantially attenuated the delayed degeneration of CA1 neurons 3 days after TFI (Fig. 2c, d). Interestingly, the neuroprotective effect of Neu2000 remained prominent 3 and 7 days post-ischemia when Neu2000 was delivered 1 day after TFI, suggesting it is the delayed phase of free radical production that contributes to DND.

Increased iron and iron regulatory protein expression in CA1 neurons following TFI

Perl's reaction with DAB intensification in sham-operated control rats revealed iron localized in the molecular layer of the dentate gyrus and mossy fibers into CA3 and weakly

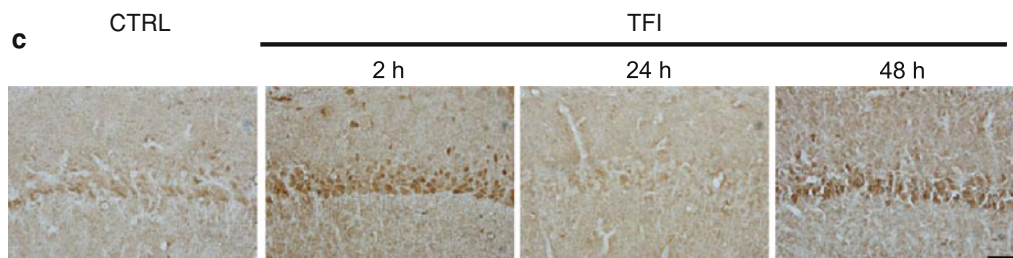
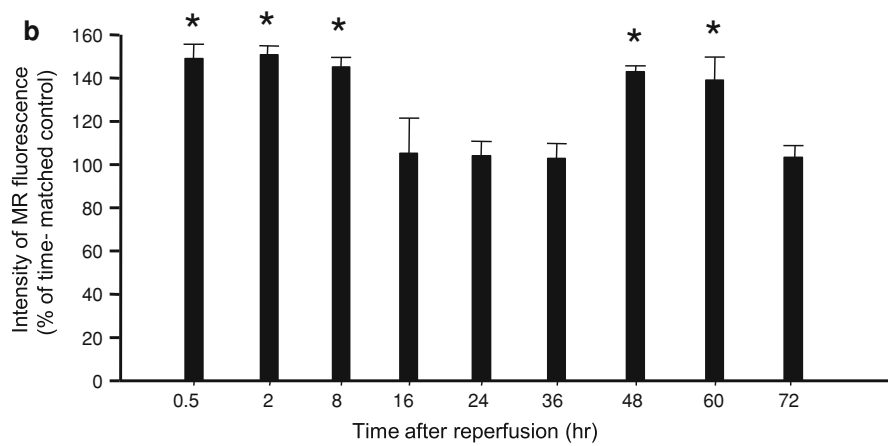
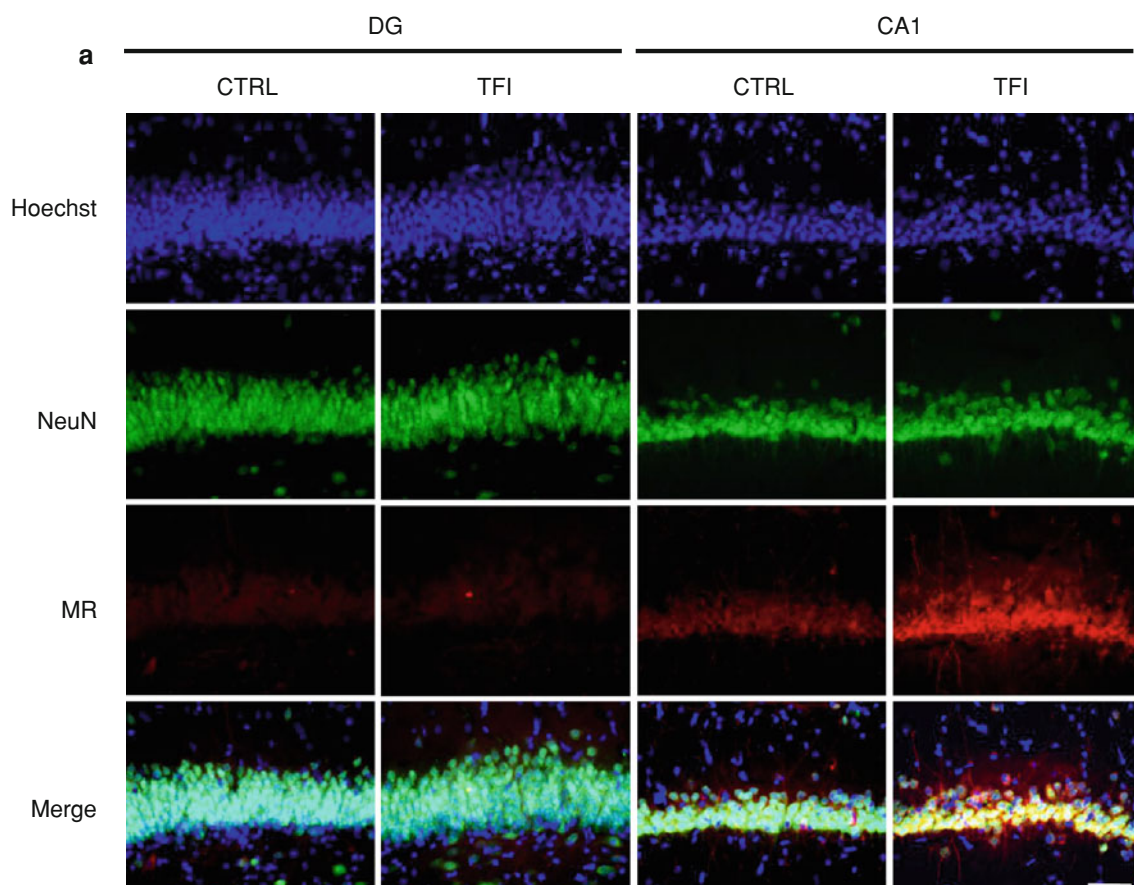
apparent in neuronal cell layers throughout the hippocampal formation. Iron intensity increased in dentate gyrus granule cells and all hippocampal pyramidal cell layers within 1 day after TFI, and remained elevated 2 days after TFI in hippocampal pyramidal cell layers but not in the dentate gyrus. Iron deposition was only observed in the CA1 pyramidal cell layer 3 days after TFI (Fig. 3a).

Additional experiments were performed to examine the iron handling proteins TfR and ferritin, which were associated with iron deposition in the CA1 after TFI (Fig. 3a). TfR was observed sparsely through the hippocampal formation in sham-operated control rats. Ferritin was observed in the molecular layer of the dentate gyrus, mossy fibers in the CA3 region, and neuronal layers of the hippocampal formation in sham-operated control rats. TfR expression markedly increased 1 day after TFI in dentate gyrus granule cells and all hippocampal cell layers including CA1, CA3, and hilar regions. The expression of TfR remained elevated in the CA1 pyramidal cell layer over the next 3 days. The expression of ferritin, an intracellular iron-sequestering protein, increased in the dentate gyrus granule cell layer and hippocampal cell layers 1 day following TFI. In contrast to TfR, however, ferritin expression in the CA1 cell layer returned to near-control levels within 2 days after TFI. Most CA1 cells immunoreactive to TfR or ferritin were labeled with the neuronal nuclear protein NeuN (Fig. 3b, c), suggesting that the expression of TfR and ferritin was increased in the CA1 pyramidal neurons 1 day following TFI.

Iron chelation with deferoxamine prevents free radical production and DND

Deferoxamine mesylate (DFO), a high-affinity chelator of  $\text{Fe}^{3+}$  ions, has been used in clinical practice for more than 30 years to remove excessive iron from the body. DFO administration (100 mg/kg, s.c.) immediately following TFI prevented the increase in intracellular iron in CA1 neurons 1 day after TFI. DFO also prevented iron overload in the CA1 subfield 7 days post-ischemia (Fig. 4a). Free radical production in CA1 neurons 2 days after TFI was completely blocked by administration of DFO (Fig. 4b), but not by Ca-EDTA, a zinc chelator, at an effective dose (100 mM, i.c.v.) previously shown to attenuate DND in the CA1 [28]. DFO (100 mg/kg, s.c) attenuated delayed degeneration of CA1 neurons following TFI. The neuroprotective effect of DFO was maintained 7 days post-ischemia (Fig. 4c).

Beneficial effects of DFO are attributed principally to its iron chelation properties, but direct radical scavenging may also be involved [19]. Therefore, we aimed to verify the iron-specific nature of the effect of DFO against free radical injury. Neuronal uptake of iron 8 h after exposure to



◀ **Fig. 1** Increase in MFR production in hippocampal CA1 neurons following TFI. **a** Fluorescence photomicrographs of cell layers in the dentate gyrus (*DG*) and hippocampal CA1 region (*CA1*) labeled with Hoechst 33258 (Hoechst), mouse anti-NeuN antibody (*NeuN*), and MitoTracker Red CM-H<sub>2</sub>XROs (*MR*) 2 h following sham operation (*CTRL*) and 10 min transient forebrain ischemia (*TFI*). Numerous punctate mitochondrial free radicals (*MFR*) were observed in hippocampal CA1 regions (*red*) and overlapped with nuclear (*blue*) and neuronal (*green*) counterstaining in the *bottom panels (Merge)*. **b** Quantitative analysis of relative intensities of MR fluorescence signals in CA1 pyramidal cells following reperfusion. MFR levels are normalized against time-matched, sham-operated controls at the indicated time points. Data are expressed as mean  $\pm$  SEM ( $n = 5$  animals for each condition). \* $P < 0.05$  compared with relevant controls, using ANOVA and Student–Newman–Keuls test. **c** Bright-field photomicrographs of CA1 sections immunolabeled with mouse anti-8-OHdG antibody in sham-operated control (*CTRL*) or ischemic rats (*TFI*) 2, 24, and 48 h following reperfusion. *Bar* 50  $\mu$ m

50  $\mu$ M FeCl<sub>2</sub> was observed in mixed cortical cell cultures of neurons and glia, which was followed by widespread neuronal death over the next 24 h (Fig. 4d). Iron uptake and neuronal death were completely blocked by concurrent administration of DFO (100  $\mu$ M). TSQ staining revealed zinc uptake in cultured cortical neurons 8 h after exposure of mixed cortical cell cultures to ZnCl<sub>2</sub> (300  $\mu$ M for 30 min). Zinc uptake and neurotoxicity were not attenuated by administration of DFO. Furthermore, DFO did not protect cells from free radical neurotoxicity induced by menadione (10  $\mu$ M), an intracellular superoxide-producing agent, or hydrogen peroxide (200  $\mu$ M) in cortical cell cultures (Fig. 4e).

TFI induces the increase of BBB permeability and iron uptake from circulating peripheral blood

Brain iron is supplemented from the blood and tightly regulated by the BBB [38], and BBB permeability has been shown to increase in brain areas sensitive to forebrain ischemia [8]. The possibility that TFI would induce BBB opening and accelerate the transport of peripheral blood iron into the brain was investigated by monitoring the extravasation of Evans blue. The fluorescent signal of Evans blue was not observed in the hippocampal formation of sham-operated control rats but increased through the brain capillary endothelium of CA1 subfields 1 day after TFI (Fig. 5a). The extravasation of Evans blue was noticeable in the dorsal hippocampus within 2 days after TFI (Fig. 5b). This implies that TFI impairs the integrity of the BBB primarily in the hippocampal formation and increases BBB permeability through the hippocampal capillary endothelium.

Additional experiments were set out to investigate if iron-containing blood cells would be infiltrated into the brain after TFI. Weak iron-positive signals were observed

in the hippocampal CA1 subfields of sham-operated control rats (Fig. 5c). The number of cells densely labeled by Perl's reaction increased in the hippocampal region including the brain capillary endothelium 1 day after TFI. The iron-positive signals were considerably reduced in rats thoroughly perfused with PBS, suggesting that iron and iron-positive cells be transported to the hippocampal areas from blood after TFI. In support of this, cells immunoreactive to MPO (a leukocyte marker) or ED2 (a macrophage marker) were increased in the hippocampal areas 1 day after TFI (Fig. 5d). Red blood cells were labeled with Glycophorine A and slightly increased around the endothelial layer. TFI also increased transferrin-positive signals through the hippocampal CA1 parenchyma.

X-ray irradiation reduces the number of leukocytes and thrombocytes in blood and TFI-induced iron overload

We performed additional experiments to examine if infiltration of blood cells such as leukocytes would be required for iron uptake and accumulation in the CA1 neurons after TFI. Perl's iron staining revealed that many iron-positive particles and cells were observed in the CA1 pyramidal cell layer and the brain capillary endothelium 1 day after TFI (Fig. 6a). TFI-induced iron overload and intensely iron-positive cells were significantly reduced in rats subjected to TFI following sublethal X-ray irradiation of the whole body except the head, which resulted in reduced number of leukocytes and thrombocytes in circulating blood (Fig. 6; Table 1). This suggests that infiltration of iron-containing blood cells to the hippocampus contributes to iron overload and iron-mediated DND in the CA1 after TFI.

## Discussion

TFI produces a biphasic pattern of free radical production in CA1 pyramidal neurons. Excess free radicals have been observed in the hippocampal formation within 30 min after TFI [46], and we confirmed these reports in our observation of mitochondrial production of free radicals in CA1 neurons 0.5–8 h after TFI. These rapidly evolving free radicals appear to be produced through multiple mechanisms involving mitochondrial dysfunction, activation of Ca<sup>2+</sup>-permeable ionotropic glutamate receptors, activation of xanthine dehydrogenase, and Zn<sup>2+</sup> accumulation after recirculation [26, 50]. Free radicals can then contribute to DND, as evident by the attenuation of neuronal loss in the CA1 by administration of the antioxidants, Neu2000 or trolox. Interestingly, MFR increase for the second time in CA1 neurons 48–60 h after TFI. Targeting these slowly evolving free radicals with delayed administration of

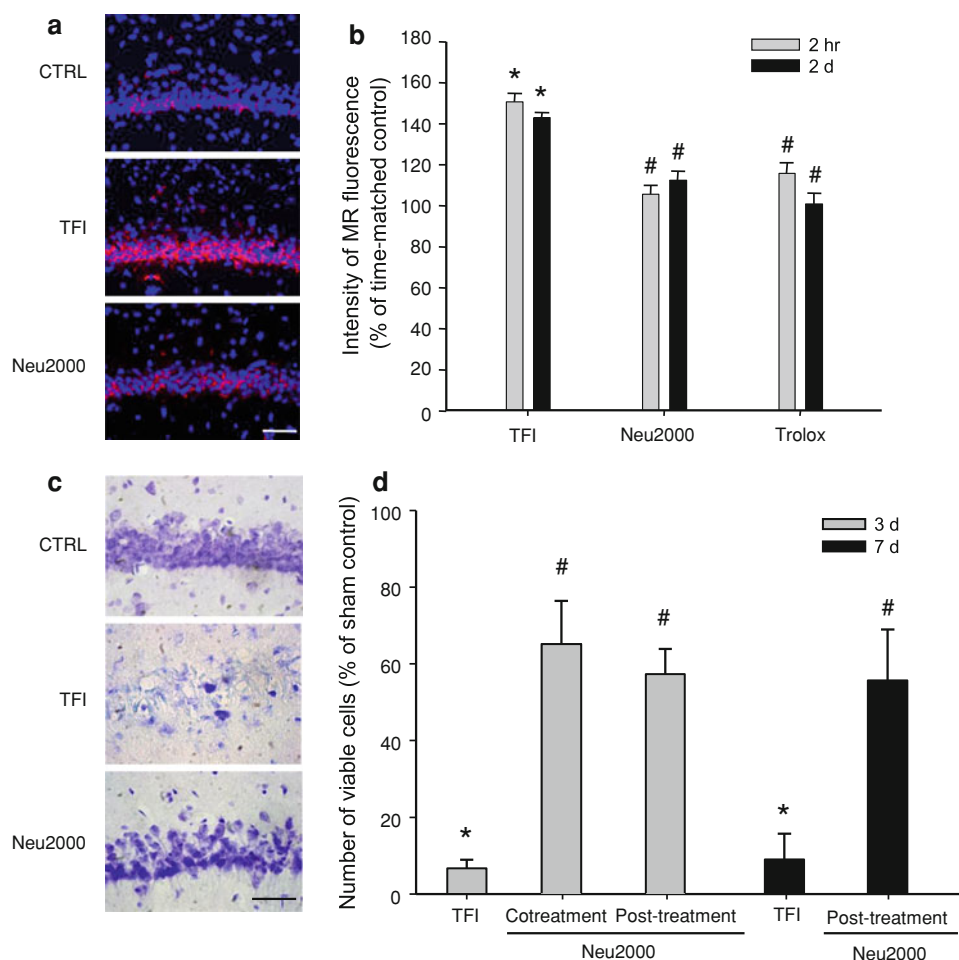


**Fig. 2** Treatment with Neu2000 attenuates TFI-induced MFR production and DND in CA1. **a** Superimposed images of fluorescence photomicrographs of hippocampal sections labeled with Hoechst 33258 and MitoTracker Red CM-H<sub>2</sub>XROs showing nuclei (blue) and MFR (red) in CA1 neurons 2 h after sham operation (CTRL), ischemia alone (TFI) or ischemia with administration of Neu2000 (50 mg/kg, i.p.) immediately after reperfusion. **b** Quantitative analysis of MFR levels in CA1 pyramidal cells 2 h or 2 days after ischemia alone (TFI) or with administration of Neu2000 (50 mg/kg, i.p.) or trolox (50 mg/kg, i.p.) immediately after reperfusion. MFR levels are normalized against time-matched, sham-operated controls at the indicated time points. Data are expressed as mean  $\pm$  SEM ( $n = 5$  animals for each condition). \* $P < 0.05$  compared with

relevant controls, # $P < 0.05$  compared with TFI, using ANOVA and Student–Newman–Keuls test. **c** Histological photomicrographs of CA1 cell layers stained with cresyl violet 3 days after reperfusion in sham-operated (CTRL), ischemic (TFI), and Neu2000-treated (TFI + Neu2000) groups. Bar 50  $\mu$ m. **d** Quantitative analysis of CA1 cell viability 3 and 7 days after reperfusion in ischemic (TFI) and Neu2000 treatment (Neu2000) groups. Neu2000 treatment protects CA1 cells against TFI-induced delayed neuronal death when was administered immediately (cotreatment) or 1 day (post-treatment) after reperfusion. Data are expressed as mean  $\pm$  SEM ( $n = 5–6$  animals for each condition). \* $P < 0.05$  compared with controls, # $P < 0.05$  compared with time-matched TFI, using ANOVA and Student–Newman–Keuls test

Neu2000 also prevented DND, suggesting that delayed free radical production contributes to TFI-induced DND.

In the present study, we demonstrated a central role of iron in mediating delayed free radical production and neuronal death in the CA1 after TFI. First, intracellular iron accumulation in CA1 neurons after TFI occurred over a prolonged period of time before delayed free radical production was observed. Second, the administration of DFO, an iron chelator, prevented both iron accumulation and delayed free radical production in CA1 neurons after TFI. Finally, DFO prevented degeneration of CA1 neurons after

TFI. The selectivity of DFO to iron was verified in cultured cortical cells, in which DFO blocked neuronal uptake of iron and iron-induced free radical neurotoxicity, but neither zinc uptake nor zinc-induced neuronal death. Moreover, DFO did not reduce neuronal death induced by the oxidants such as H<sub>2</sub>O<sub>2</sub> or menadione.

Iron is bound to a high-affinity Fe<sup>3+</sup> binding site of transferrin, which is then acquired by target cells through TfR-mediated endocytosis [37]. TfR expression correlates with cellular iron uptake and has been reported to increase in ischemic tissue after reperfusion [56], indicating that



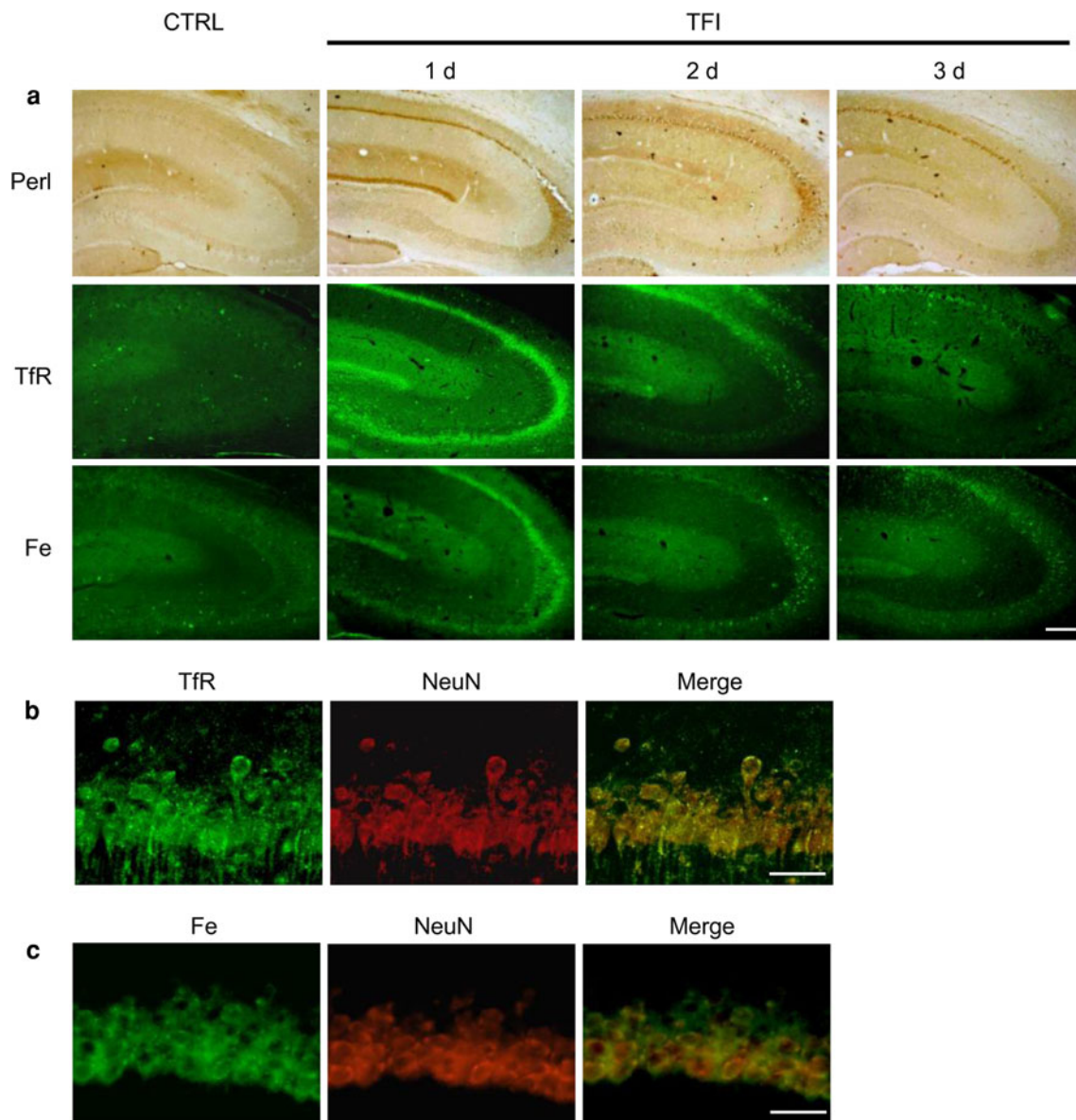


**Fig. 3** Iron distribution and expression of transferrin receptor and ferritin in the hippocampal formation following TFI. **a.** Histological photomicrographs of hippocampal sections with Perl's iron staining in sham-operated control (*CTRL*) and ischemic rats (*TFI*) 1–3 days following reperfusion (*top panel*). Fluorescence photomicrographs showing hippocampal sections immunolabeled with mouse anti-transferrin receptor (*TfR*, *middle panel*) and rabbit anti-ferritin (*Fe*,

*bottom panel*) antibodies in sham-operated control (*CTRL*) and ischemic rats (*TFI*) 1–3 days following reperfusion. *Bar* 250  $\mu$ m. **b–c** Fluorescence photomicrographs of the NeuN-positive CA1 neurons (*red*) colocalized with transferrin receptor (*TfR*) (**b**, *green*) or ferritin (*Fe*) (**c**, *green*) 1 day after TFI. Note upregulation of TfR and Fe in CA neurons (*Merge*, *yellow*). *Bar* 50  $\mu$ m

TFI-induced iron overload in CA1 neurons likely involves upregulation of TfR, which is located primarily on endothelial cells and oligodendrocytes in the nervous system [14]. TfR expression increased in hippocampal CA1–CA3 neurons within 1 day after TFI and remained elevated in CA1 neurons 3 days after TFI. The expression pattern of TfR correlated well with the presence of iron overload in the hippocampus. Expression of ferritin, an iron-sequestering protein, was also increased in hippocampal neurons within 1 day after TFI but returned to control levels 2 days

later, suggesting that iron is taken up by CA1 neurons through TfR-mediated endocytosis and present possibly in a free form unbound to ferritin at 2 days. These findings imply that the excess of iron uptake and the lack of iron stores might promote the accumulation of intracellular free iron, which results in the second production of toxic free radicals through iron-mediated Fenton reaction. Further study will be needed to delineate the molecular mechanisms underlying selective and temporal regulation of TfR and ferritin in the hippocampus after TFI.

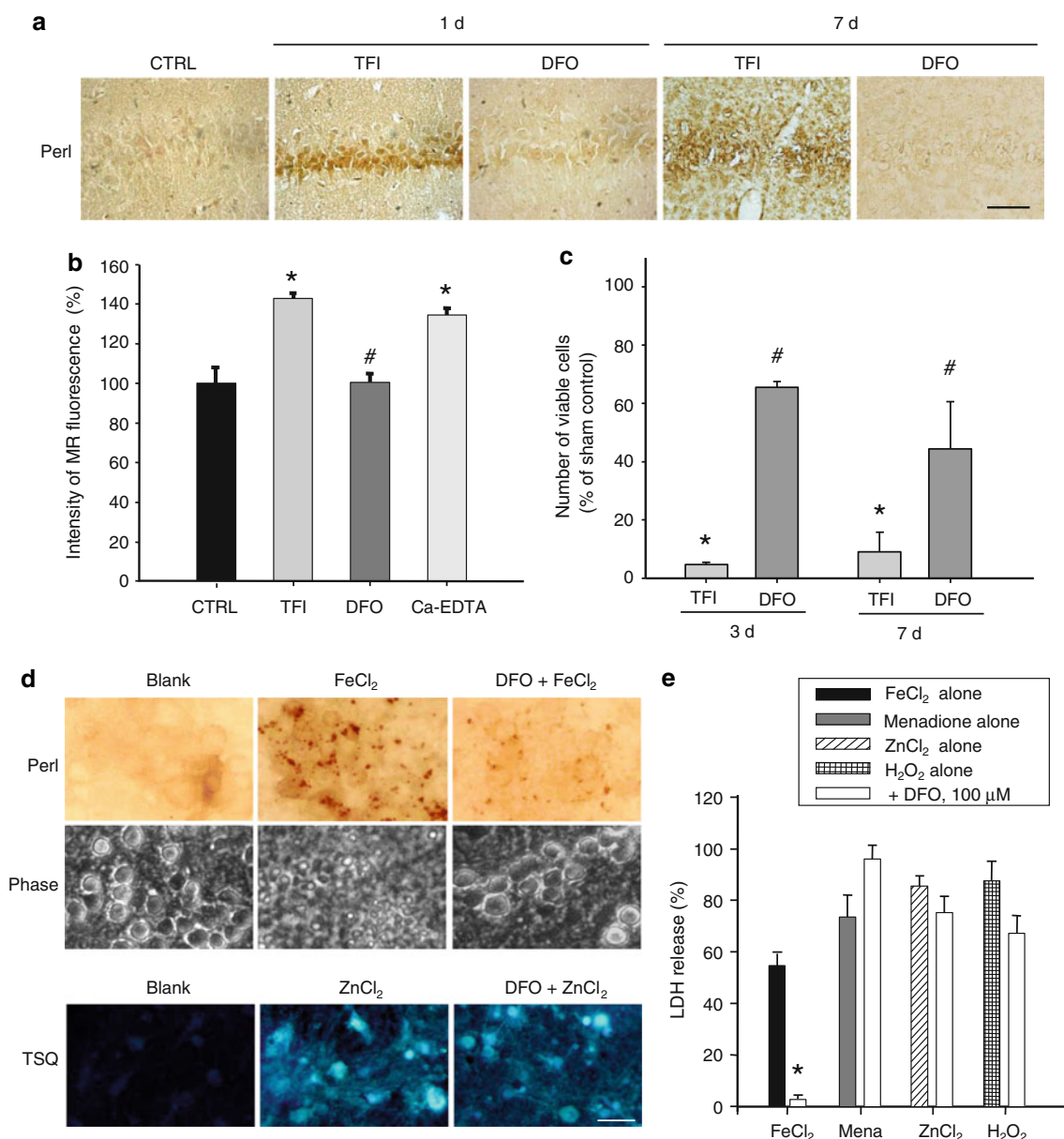


**Fig. 4** Iron mediates TFI-induced MFR production and DND in CA1. **a** Histological photomicrographs of hippocampal sections with Perl's iron staining 1 and 7 days after sham operation (*CTRL*), ischemia (*TFI*), or with administration of deferoxamine (*DFO*, 100 mg/kg s.c.) immediately after reperfusion. Bar 50 μm. **b** Quantitative analysis of MFR levels in CA1 pyramidal cells 2 days after ischemia (*TFI*) or with administration of *DFO* (100 mg/kg s.c.), Ca-EDTA (100 mM, i.c.v.) immediately after reperfusion, normalized to sham-operated control (*CTRL*). Data are expressed as mean ± SEM ( $n = 5$  animals for each condition). \* $P < 0.05$  compared with controls, # $P < 0.05$  compared with *TFI*, using ANOVA and Student–Newman–Keuls test. **c** Quantitative analysis of CA1 cell viability 3 and 7 days after ischemia (*TFI*) or with administration of *DFO* (100 mg/kg, s.c.). Data are expressed as mean ± SEM ( $n = 5$ –6 animals for each condition). \* $P < 0.05$  compared with controls, # $P < 0.05$  compared with *TFI*. **d** Bright-field

photomicrographs (*top panel*) after Perl's staining at 8 h and phase contrast photomicrographs (*middle panel*) 24 h following continuous exposure of cultured cortical cells to sham wash (*Blank*) or 50 μM FeCl<sub>2</sub>, alone or with inclusion of 100 μM *DFO* (*DFO + FeCl<sub>2</sub>*). Fluorescence photomicrographs (*bottom panel*) of cortical cells with TSQ staining for zinc deposition 8 h following exposure to sham wash (*Blank*) or 300 μM ZnCl<sub>2</sub> for 30 min, alone or with inclusion of 100 μM *DFO* (*DFO + ZnCl<sub>2</sub>*). Bar 25 μm. **e** The protective effect of *DFO* against free radical injury was analyzed by measuring LDH efflux into the bathing media of mouse cortical cell cultures (12–14 DIV) 24 h following exposure to 50 μM FeCl<sub>2</sub>, 10 μM menadione (*Mena*), 200 μM H<sub>2</sub>O<sub>2</sub> continuously, or 300 μM ZnCl<sub>2</sub> for 30 min, alone or with inclusion of 100 μM *DFO*. Data are expressed as mean ± SEM ( $n = 7$ –12 culture wells per condition). \* $P < 0.05$ , compared with FeCl<sub>2</sub>, menadione, H<sub>2</sub>O<sub>2</sub>, or ZnCl<sub>2</sub> alone

Levels of iron in the nervous system have been reported to remain constant under normal conditions, possibly due to the tight regulation of iron entry through

the BBB [3]. However, iron homeostasis can be disrupted under certain pathological conditions that compromise the BBB. In particular, ischemic brain injury renders the BBB

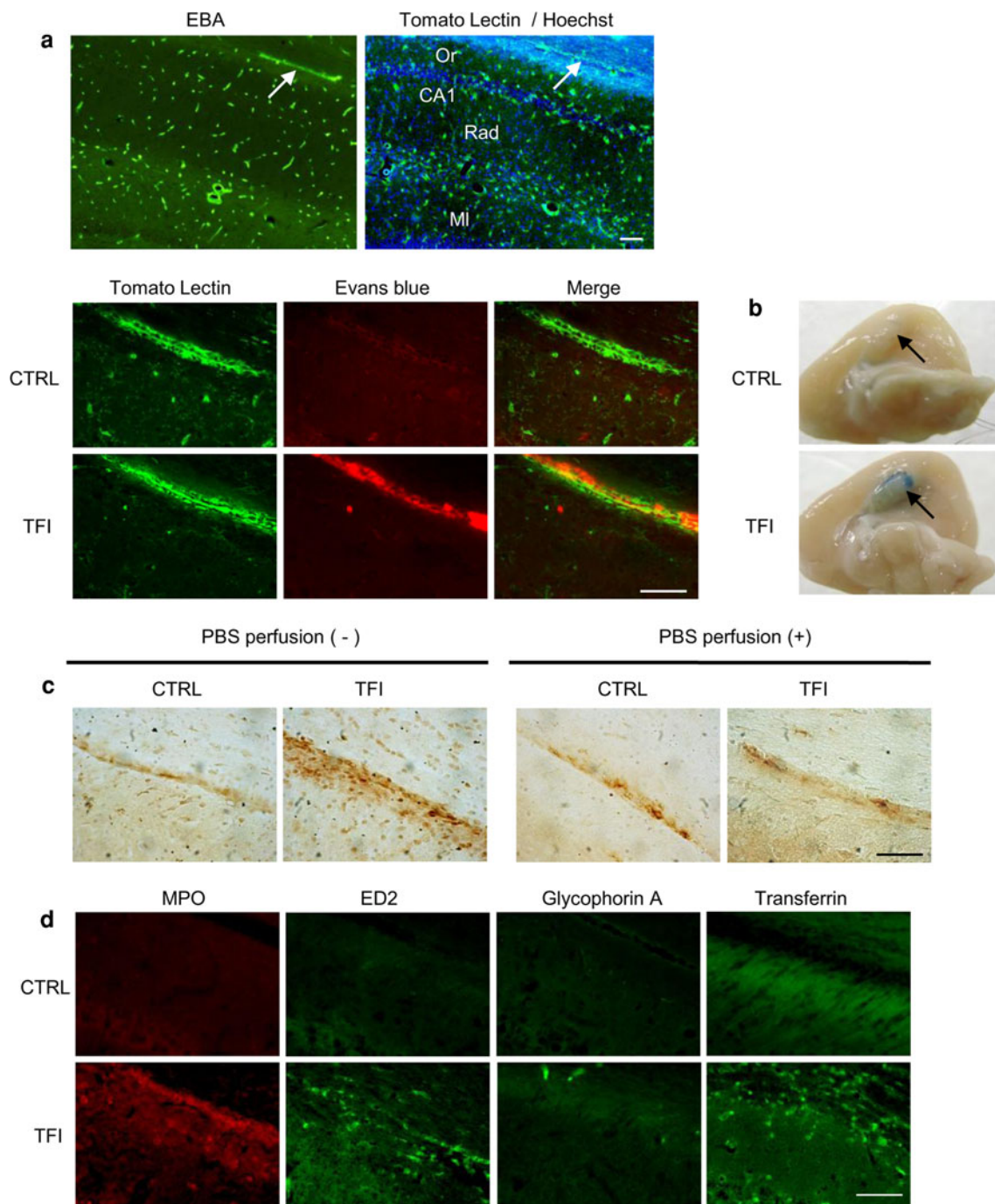


**Fig. 5** Increased BBB permeability and infiltration of circulating blood cells following TFI. **a** *Top panel* Low power fluorescent photomicrographs showing capillary endothelium (*arrows*) in the hippocampal CA1 subfields after labeling with an anti-endothelial barrier antigen (EBA) antibody or fluorescein-*Lycopersicon esculentum* (Tomato) Lectin (*green*) overlaid with Hoechst 33258 (*blue*). *Bottom panel* High power fluorescent photomicrographs showing EBD signals (*red*) double labeled with fluorescein-*Lycopersicon esculentum* (Tomato) Lectin (*green*) at brain capillary endothelium 1 day after sham operation (*CTRL*) or TFI. *Or* oriens, *Rad* radiatum,

*Ml* molecular layers. **b** Representative photographs showing the Evans blue extravasations (*blue*) in the dorsal hippocampus (*arrow*) in mid-sagittal planes of rat brains 2 days after sham operation (*CTRL*) or TFI. **c** Histological photomicrographs of the CA1 subfields subjected to Perl's staining with (+) or without (-) PBS perfusion 1 day following sham operation (*CTRL*) or TFI. **d** Fluorescent photomicrographs of the brain capillary endothelium of the CA1 subfields showing infiltration of leukocytes stained with MPO, macrophages stained with ED2, erythrocytes stained with glycophorin A, and transferrin (*green*). *Bar* 50  $\mu$ m

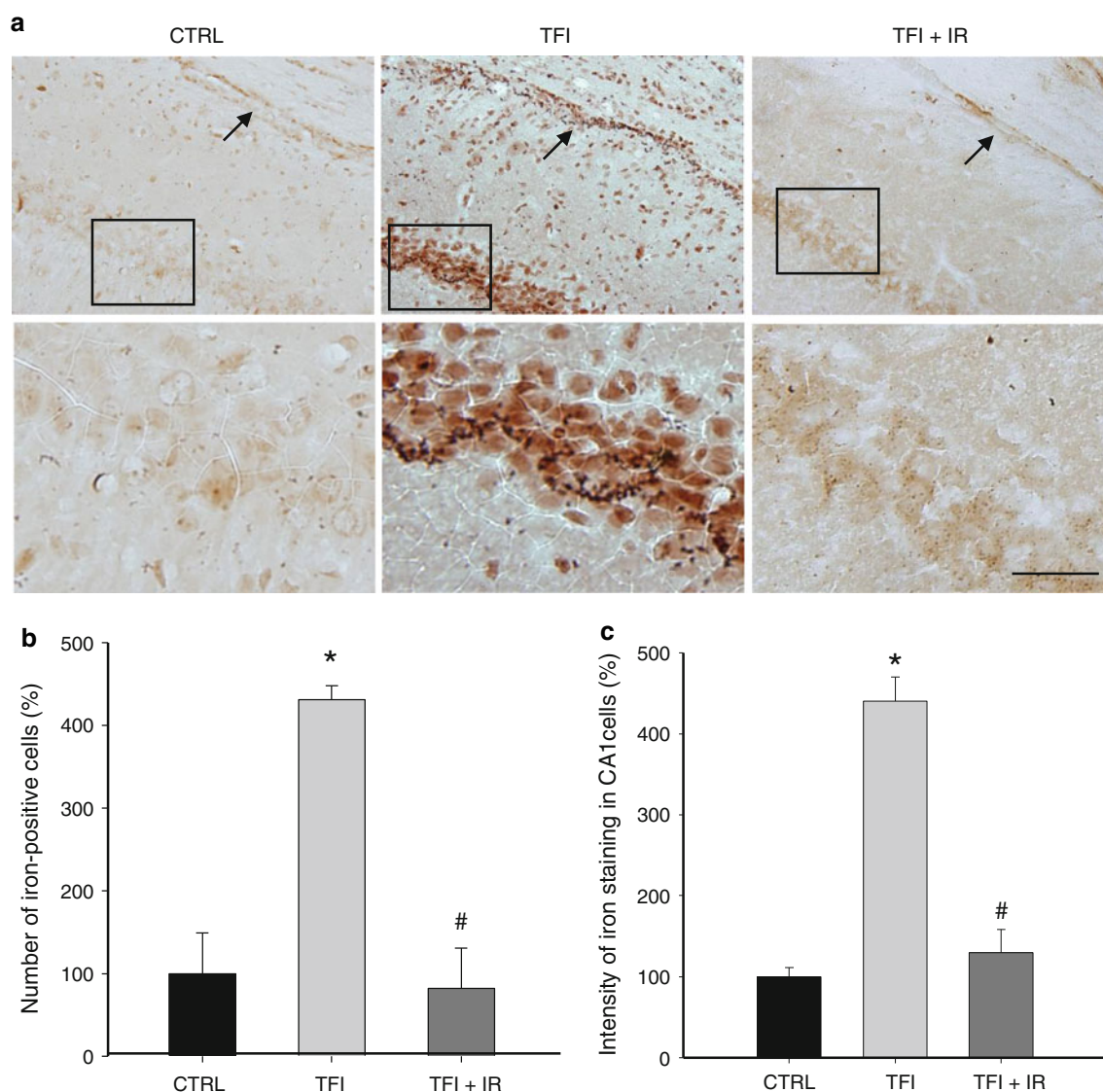


**Fig. 6** Infiltration of iron-containing blood cells contributes to iron overload in CA1 cells. **a** Histological photomicrographs of CA1 subfields (arrows brain capillary endothelium, square CA1 pyramidal cell layer) labeled with Perl's iron staining 1 day after sham operation (CTRL) or TFI, alone (TFI) or with X-ray irradiation (TFI + IR). Note that irradiation prevents TFI-induced iron overload in CA1 cells

(bottom panel high-magnification images of squared areas). Bar 50  $\mu\text{m}$ . **b**, **c** Infiltration of iron-containing cells was analyzed by counting cells positive with Perl's staining in CA1 subfields (**b**) and iron intensity measured in CA1 cells (**c**) ( $n = 5$  animals for each condition). \* $P < 0.05$  compared to CTRL, # $P < 0.05$  compared to TFI

highly permeable to metals, macromolecules, and blood cells [12, 13], resulting in abnormal infiltration of iron and iron-containing cells into brain areas undergoing TFI-induced weakening of the BBB. In the present study, infiltration of siderotic granules and iron-stained cells from blood was observed in the hippocampus after TFI, which, along with iron overload in CA1 neurons, was attenuated in irradiated rats with substantially reduced blood cell counts. Taken together, our findings indicate that iron uptake by hippocampal neurons after TFI may stem from iron-containing blood cells.

Chemoattractants mediate leukocyte recruitment to sites of injury and infection under various pathological conditions [10]. Neutrophils and macrophages are recruited into injured brain areas after focal cerebral ischemia, which is significantly reduced in monocyte chemoattractant protein 1 (MCP-1)-deficient mice [52]. Expression of MCP-1 and macrophage inflammatory protein-1-alpha (MIP-1-alpha) is increased in CA1 neurons after TFI and thought to mediate the recruitment of iron-containing infiltrating leukocytes and possibly erythrocytes [57]. Iron can be released from these recruited blood cells and then iron-

**Table 1** Blood cell counts in normal and irradiated rats

Blood cell type	Parameter (unit)	Control	IR	<i>P</i> value
Leukocytes	WBC (K/ $\mu$ l)	10.91 $\pm$ 2.58	0.88 $\pm$ 0.23	0.00
	NE (K/ $\mu$ l)	2.44 $\pm$ 0.68	0.49 $\pm$ 0.16	0.01
	LY (K/ $\mu$ l)	7.70 $\pm$ 1.77	0.48 $\pm$ 0.08	0.00
	MO (K/ $\mu$ l)	0.67 $\pm$ 0.18	0.07 $\pm$ 0.02	0.00
	EO (K/ $\mu$ l)	0.08 $\pm$ 0.04	0.01 $\pm$ 0.005	0.01
	BA (K/ $\mu$ l)	0.22 $\pm$ 0.01	0.004 $\pm$ 0.003	0.02
Erythrocytes	RBC (M/ $\mu$ l)	4.91 $\pm$ 0.65	3.29 $\pm$ 0.66	0.92
	Hb (g/dl)	10.04 $\pm$ 1.45	6.82 $\pm$ 1.49	0.91
	HCT (%)	29.51 $\pm$ 4.07	20.39 $\pm$ 4.35	0.84
Thrombocytes	PLT (K/ $\mu$ l)	422.4 $\pm$ 115.06	135.2 $\pm$ 49.68	0.01

Blood samples were collected from the femoral vein of normal control rats (control) and rats 5 days after irradiation (IR). Blood cells were counted using a Hemavet 950 FS (Drew Scientific Inc.). Data are expressed as mean  $\pm$  SEM. Statistical analysis was performed using Student's *t* test

WBC white blood cell, NE neutrocyte, LY lymphocyte, MO monocyte, EO eosinophil, BA basophil, RBC red blood cell, Hb hemoglobin, HCT hematocrit, PLT platelet

transferrin is taken up by and accumulates in CA1 neurons over-expressing TfR for a prolonged period of time after TFI. Excessive iron uptake and elevation of free iron in CA1 neurons produces OH $\cdot$  radicals at delayed second phase and appears to trigger DND after TFI.

In conclusion, the present findings suggest that deregulation of neuronal iron homeostasis triggers the formation of slowly evolving free radicals in an iron overload-dependent manner in CA1. This loss of iron homeostasis possibly results from a molecular and cellular cascade, including prolonged upregulation of TfR and brain infiltration of iron-containing blood cells and siderotic granules from the circulating blood through a compromised BBB. Iron and iron-catalyzed  $\cdot$ OH radicals then contribute to DND in the CA1 region after TFI. A time window for neuroprotection with antioxidants is present up to 24 h after TFI, indicating that timely intervention with antioxidants may attenuate neuronal death in human patients with forebrain ischemia or cardiac arrest.

**Acknowledgments** This work was supported by grants from the Brain Korea 21 Project for Medical Science, Ajou University, the 21C Frontier R&D Program in Neuroscience from Ministry of Education, Science and Technology, and Neurotech Pharmaceuticals.

**Conflict of interest** UJP, YAL, JHL, and BJG are employees of Neurotech Pharmaceuticals. SMW, SK, JES, and YBL have no conflict of interest.

## References

- Alam ZI, Jenner A, Daniel SE et al (1997) Oxidative DNA damage in the parkinsonian brain: an apparent selective increase in 8-hydroxyguanine levels in substantia nigra. *J Neurochem* 69:1196–1203
- Bennett MV, Pellegrini-Giampietro DE, Gorter JA, Aronica E, Connor JA, Zukin RS (1996) The GluR2 hypothesis: Ca(++)-permeable AMPA receptors in delayed neurodegeneration. *Cold Spring Harb Symp Quant Biol* 61:373–384
- Bradbury MW (1997) Transport of iron in the blood–brain–cerebrospinal fluid system. *J Neurochem* 69:443–454
- Calderone A, Jover T, Mashiko T et al (2004) Late calcium EDTA rescues hippocampal CA1 neurons from global ischemia-induced death. *J Neurosci* 24:9903–9913
- Carbonell T, Rama R (2007) Iron, oxidative stress and early neurological deterioration in ischemic stroke. *Curr Med Chem* 14:857–874
- Chan PH, Kawase M, Murakami K et al (1998) Overexpression of SOD1 in transgenic rats protects vulnerable neurons against ischemic damage after global cerebral ischemia and reperfusion. *J Neurosci* 18:8292–8299
- Cherubini A, Ruggiero C, Polidori MC, Mecocci P (2005) Potential markers of oxidative stress in stroke. *Free Radic Biol Med* 39:841–852
- Dobbin J, Crockard HA, Ross-Russell R (1989) Transient blood–brain barrier permeability following profound temporary global ischaemia: an experimental study using 14C-AIB. *J Cereb Blood Flow Metab* 9:71–78
- Eichmüller S, Stevenson PA, Paus R (1996) A new method for double immunolabelling with primary antibodies from identical species. *J Immunol Methods* 190:255–265
- Frangogiannis NG (2007) Chemokines in ischemia and reperfusion. *Thromb Haemost* 97:738–747
- Frederickson CJ, Hernandez MD, McGinty JF (1989) Translocation of zinc may contribute to seizure-induced death of neurons. *Brain Res* 480:317–321
- Garcia JH, Liu KF, Yoshida Y, Lian J, Chen S, del Zoppo GJ (1994) Influx of leukocytes and platelets in an evolving brain infarct (Wistar rat). *Am J Pathol* 144:188–199
- Gidday JM, Gasche YG, Copin JC et al (2005) Leukocyte-derived matrix metalloproteinase-9 mediates blood–brain barrier breakdown and is proinflammatory after transient focal cerebral ischemia. *Am J Physiol Heart Circ Physiol* 289:H558–H568
- Giometto B, Bozza F, Argentiero V et al (1990) Transferrin receptors in rat central nervous system. An immunocytochemical study. *J Neurol Sci* 98:81–90

15. Gorter JA, Petrozzino JJ, Aronica EM et al (1997) Global ischemia induces downregulation of GluR2 mRNA and increases AMPA receptor-mediated Ca<sup>2+</sup> influx in hippocampal CA1 neurons of gerbil. *J Neurosci* 17:6179–6188
16. Gupta S, Sharma SS (2006) Neuroprotective effects of trolox in global cerebral ischemia in gerbils. *Biol Pharm Bull* 29: 957–961
17. Gwag BJ, Koh JY, DeMaro JA, Ying HS, Jacquin M, Choi DW (1997) Slowly triggered excitotoxicity occurs by necrosis in cortical cultures. *Neuroscience* 77:393–401
18. Gwag BJ, Lee YA, Ko SY et al (2007) Marked prevention of ischemic brain injury by Neu2000, an NMDA antagonist and antioxidant derived from aspirin and sulfasalazine. *J Cereb Blood Flow Metab* 27:1142–1151
19. Halliwell B (1989) Protection against tissue damage in vivo by desferrioxamine: what is its mechanism of action? *Free Radic Biol Med* 7:645–651
20. Hara H, Kato H, Kogure K (1990) Protective effect of alpha-tocopherol on ischemic neuronal damage in the gerbil hippocampus. *Brain Res* 510:335–338
21. He K, Aizenman E (2010) ERK signaling leads to mitochondrial dysfunction in extracellular zinc-induced neurotoxicity. *J Neurochem* 114:452–461
22. Hill JM, Switzer RC 3rd (1984) The regional distribution and cellular localization of iron in the rat brain. *Neuroscience* 11:595–603
23. Kane PJ, Modha P, Strachan RD et al (1992) The effect of immunosuppression on the development of cerebral oedema in an experimental model of intracerebral haemorrhage: whole body and regional irradiation. *J Neurol Neurosurg Psychiatry* 55:781–786
24. Ke Y, Ming Qian Z (2003) Iron misregulation in the brain: a primary cause of neurodegenerative disorders. *Lancet Neurol* 2:246–253
25. Kim DY, Won SJ, Gwag BJ (2002) Analysis of mitochondrial free radical generation in animal models of neuronal disease. *Free Radic Biol Med* 33:715–723
26. Kim EY, Koh JY, Kim YH, Sohn S, Joe E, Gwag BJ (1999) Zn<sup>2+</sup> entry produces oxidative neuronal necrosis in cortical cell cultures. *Eur J Neurosci* 11:327–334
27. Kirino T, Tamura A, Sano K (1984) Delayed neuronal death in the rat hippocampus following transient forebrain ischemia. *Acta Neuropathol* 64:139–147
28. Koh JY, Suh SW, Gwag BJ, He YY, Hsu CY, Choi DW (1996) The role of zinc in selective neuronal death after transient global cerebral ischemia. *Science* 272:1013–1016
29. Kompala SD, Babbs CF, Blaho KE (1986) Effect of deferoxamine on late deaths following CPR in rats. *Ann Emerg Med* 15:405–407
30. Kondo Y, Ogawa N, Asanuma M, Ota Z, Mori A (1995) Regional differences in late-onset iron deposition, ferritin, transferrin, astrocyte proliferation, and microglial activation after transient forebrain ischemia in rat brain. *J Cereb Blood Flow Metab* 15:216–226
31. Lee DW, Andersen JK, Kaur D (2006) Iron dysregulation and neurodegeneration: the molecular connection. *Mol Interv* 6:89–97
32. LeVine SM (1997) Iron deposits in multiple sclerosis and Alzheimer's disease brains. *Brain Res* 760:298–303
33. Liu G, Garrett MR, Men P, Zhu X, Perry G, Smith MA (2005) Nanoparticle and other metal chelation therapeutics in Alzheimer disease. *Biochim Biophys Acta* 1741:246–252
34. Lovell MA, Markesbery WR (2001) Ratio of 8-hydroxyguanine in intact DNA to free 8-hydroxyguanine is increased in Alzheimer disease ventricular cerebrospinal fluid. *Arch Neurol* 58:392–396
35. Medvedeva YV, Lin B, Shuttleworth CW, Weiss JH (2009) Intracellular Zn<sup>2+</sup> accumulation contributes to synaptic failure, mitochondrial depolarization, and cell death in an acute slice oxygen-glucose deprivation model of ischemia. *J Neurosci* 29:1105–1114
36. Montine KS, Quinn JF, Zhang J et al (2004) Isoprostanes and related products of lipid peroxidation in neurodegenerative diseases. *Chem Phys Lipids* 128:117–124
37. Moos T, Morgan EH (2000) Transferrin and transferrin receptor function in brain barrier systems. *Cell Mol Neurobiol* 20:77–95
38. Moos T (2002) Brain iron homeostasis. *Dan Med Bull* 49:279–301
39. Moos T, Morgan EH (2004) The metabolism of neuronal iron and its pathogenic role in neurological disease: review. *Ann N Y Acad Sci* 1012:14–26
40. Nagaraja TN, Keenan KA, Fenstermacher JD, Knight RA (2008) Acute leakage patterns of fluorescent plasma flow markers after transient focal cerebral ischemia suggest large openings in blood-brain barrier. *Microcirculation* 15:1–14
41. Nayini NR, White BC, Aust SD et al (1985) Post resuscitation iron delocalization and malondialdehyde production in the brain following prolonged cardiac arrest. *J Free Radic Biol Med* 1:111–116
42. Noh KM, Yokota H, Mashiko T, Castillo PE, Zukin RS, Bennett MV (2005) Blockade of calcium-permeable AMPA receptors protects hippocampal neurons against global ischemia-induced death. *Proc Natl Acad Sci USA* 102:12230–12235
43. Pagnussat AS, Faccioni-Heuser MC, Netto CA, Achaval M (2007) An ultrastructural study of cell death in the CA1 pyramidal field of the hippocampus in rats submitted to transient global ischemia followed by reperfusion. *J Anat* 211:589–599
44. Palmer C, Menzies SL, Roberts RL, Pavlick G, Connor JR (1999) Changes in iron histochemistry after hypoxic-ischemic brain injury in the neonatal rat. *J Neurosci Res* 56:60–71
45. Pellegrini-Giampietro DE, Gorter JA, Bennett MV, Zukin RS (1997) The GluR2 (GluR-B) hypothesis: Ca<sup>2+</sup>-permeable AMPA receptors in neurological disorders. *Trends Neurosci* 20:464–470
46. Piantadosi CA, Zhang J (1996) Mitochondrial generation of reactive oxygen species after brain ischemia in the rat. *Stroke* 27:327–331 (discussion 32)
47. Deng P, Xu ZC (2009) Four-vessel occlusion model in rats. In: Chen J, Xu ZC, Xu X-M et al (eds) *Animal models of acute neurological injuries*, Humana Press, Clifton, pp 65–76
48. Pulsinelli WA, Brierley JB (1979) A new model of bilateral hemispheric ischemia in the unanesthetized rat. *Stroke* 10:267–272
49. Pulsinelli WA (1985) Selective neuronal vulnerability: morphological and molecular characteristics. *Prog Brain Res* 63:29–37
50. Rodrigo J, Fernandez AP, Serrano J, Peinado MA, Martinez A (2005) The role of free radicals in cerebral hypoxia and ischemia. *Free Radic Biol Med* 39:26–50
51. Rosenthal RE, Chanderbhan R, Marshall G, Fiskum G (1992) Prevention of post-ischemic brain lipid conjugated diene production and neurological injury by hydroxyethyl starch-conjugated deferoxamine. *Free Radic Biol Med* 12:29–33
52. Schilling M, Strecker JK, Schabitz WR, Ringelstein EB, Kiefer R (2009) Effects of monocyte chemoattractant protein 1 on blood-borne cell recruitment after transient focal cerebral ischemia in mice. *Neuroscience* 161:806–812
53. Selim MH, Ratan RR (2004) The role of iron neurotoxicity in ischemic stroke. *Ageing Res Rev* 3:345–353
54. Sheardown MJ, Suzdak PD, Nordholm L (1993) AMPA, but not NMDA, receptor antagonism is neuroprotective in gerbil global ischaemia, even when delayed 24 h. *Eur J Pharmacol* 236:347–353

55. Sugawara T, Noshita N, Lewen A et al (2002) Overexpression of copper/zinc superoxide dismutase in transgenic rats protects vulnerable neurons against ischemic damage by blocking the mitochondrial pathway of caspase activation. *J Neurosci* 22:209–217
56. Tacchini L, Fusar Poli D, Bernelli-Zazzera A, Cairo G (2002) Transferrin receptor gene expression and transferrin-bound iron uptake are increased during postischemic rat liver reperfusion. *Hepatology* 36:103–111
57. Wang HK, Park UJ, Kim SY et al (2008) Free radical production in CA1 neurons induces MIP-1alpha expression, microglia recruitment, and delayed neuronal death after transient forebrain ischemia. *J Neurosci* 28:1721–1727
58. White BC, Krause GS, Aust SD, Eyster GE (1985) Postischemic tissue injury by iron-mediated free radical lipid peroxidation. *Ann Emerg Med* 14:804–809
59. Winkelmann ER, Charcansky A, Faccioni-Heuser MC, Netto CA, Achaval M (2006) An ultrastructural analysis of cellular death in the CA1 field in the rat hippocampus after transient forebrain ischemia followed by 2, 4 and 10 days of reperfusion. *Anat Embryol (Berl)* 211:423–434
60. Yoshidomi M, Hayashi T, Abe K, Kogure K (1989) Effects of a new calcium channel blocker, KB-2796, on protein synthesis of the CA1 pyramidal cell and delayed neuronal death following transient forebrain ischemia. *J Neurochem* 53:1589–1594
61. Youdim MB, Stephenson G, Ben Shachar D (2004) Ironing iron out in Parkinson's disease and other neurodegenerative diseases with iron chelators: a lesson from 6-hydroxydopamine and iron chelators, desferal and VK-28. *Ann NY Acad Sci* 1012:306–325